DOI : https://doi.org/10.7186/wg521202602

Rare earth element enrichment in the southern part of Taiping pluton

Ibrahim Danial Maarof*, Nor Syazwani Zainal Abidin, Belinda Clare Bonny

Geoscience Department, Faculty of Science, Universiti Teknologi PETRONAS, 32610, Seri Iskandar, Perak, Malaysia
*Corresponding author email address: ibrahim.maarof@yahoo.com

Abstract: This study investigates rare earth elements (REE) occurrences in the southern part of Taiping pluton, part of Bintang batholith in Peninsular Malaysia. 36 samples were collected from three outcrops (PSS, PUK, MJ) across four weathering horizons (A, B, C, D) and analysed using X-ray fluorescence (XRF), X-ray diffraction (XRD), petrography and inductively coupled plasma mass spectrometry (ICP-MS). The granitic bedrock (horizon D) is amphibole-bearing I-type granite, averaging 389.00 ppm REE. The granite was observed containing zircon and apatite as the main REE-bearing minerals. Among the weathered profiles, horizon C shows the highest enrichment, averaging 683.00 ppm, compared with 258.00 ppm in horizon B and 119.75 ppm in horizon A. The strong enrichment of REE occurred in horizon C due to the closer depth to the granite and REMs. This finding provides new insight for the enrichment of REE within the weathered profiles of Taiping pluton.

Keywords: REE, Main Range Granite, Bintang batholith, Taiping pluton, geochemical

Abstrak: Kajian ini menyiasat kehadiran unsur-unsur nadir bumi (REE) di bahagian selatan pluton Taiping, yang merupakan sebahagian daripada batolit Bintang di Semenanjung Malaysia. Sebanyak 36 sampel telah diambil dari tiga singkapan (PSS, PUK, MJ) yang merentasi empat lapisan luluhawa (A, B, C, D) dan telah dianalisa menggunakan pendarfluor sinar-X (XRF), pembelauan sinar-X (XRD), petrografi, dan ICP-MS. Batuan dasar (lapisan D) adalah granit jenis-I yang mengandungi amfibol, dengan purata 389.00 ppm REE. Batuan dasar ini mengandungi zircon dan apatit sebagai mineral utama pembawa REE. Antara lapisan – lapisan profil terluluhawa yang terbentuk di lapangan, lapisan C mempunyai pengayaan yang tertinggi, dengan purata 683.00 ppm, berbanding 258.00 ppm di lapisan B dan 119.75 ppm di lapisan A. Pengayaan REE yang tinggi berlaku di lapisan C disebabkan oleh kedalaman yang lebih hampir dengan batuan dasar dan mineral nadir bumi (REMs). Penemuan ini memberikan pandangan baharu untuk pengayaan REE dalam profil terluluhawa pluton Taiping.

Kata kunci: REE, Granit Banjaran Utama, batolit Bintang, pluton Taiping, geokimia

INTRODUCTION

Background

Rare earth elements (REE) comprise of seventeen elements in the periodic table, of which fifteen are from the lanthanide group and the remaining are scandium (Sc) and yttrium (Y). REE have emerged as critical components in modern technologies such as renewable energy systems, electronics and defence applications. This growing importance has become the drive factor for researchers to develop sustainable extraction strategies (Ibad *et al*., 2024). Among a few deposit types of REE, ion – adsorption clay deposits are getting attention due to their lower environmental impact during mining, which involves non – radioactive leaching processes.

REE can be commonly found in higher concentrations within some specific geological environments. These include alkaline and peralkaline igneous rocks, carbonatite intrusions, as well as certain sedimentary formations (Haxel *et al*., 2002). Under Malaysia's moist and warm climate, with consistently uniform temperatures throughout the year (Malaysian Meteorological Department, 2025), bedrocks undergo intense weathering processes that contribute to the breakdown of REE – enriched minerals or also known as Rare Earth Minerals (REM). Released REE from the REM are typically mobilised in ionic state and subsequently adsorbed to the weathering products of host rocks, particularly clay minerals. Over time, this process leads to the ion-adsorption clay-type deposits,

0126-5539; 2682-7549 / Published by the Geological Society of Malaysia.

which can develop into economically valuable secondary source of REE (Mouchos *et al*., 2017).

Previous studies

Malaysian granite plutons, especially the Taiping pluton, were previously studied by Ghani (2005); Ghani *et al*. (2013) and Quek *et al*. (2015, 2016, 2017). Taiping pluton is found to be a large, elongated igneous body that stretches from Kupang in Kedah to Beruas in Perak (Figure 1). Geologically, studies conducted by Ghani *et al*. (2013) and Husin *et al*. (2015), found that Taiping granite complex is one of prime examples for amphibole – bearing granite with large crystal sizes and prominent K – feldspar phenocrysts. It also exhibits a strong flow alignment and research by Quek *et al*. (2016) found that the amphibole content varies from accessory to minor, containing more than 1000 ppm of total rare earth elements (TREE) concentration (Quek *et al*., 2017).

The (Akademi Sains Malaysia, 2014) initiated a study on REE hosted in ion-adsorption clay-type deposits, with particular focus on HREE derived from granite weathering products. The behaviour of REE in chemically weathered granites, especially in tropical environments, are not widely documented and poorly understood (Mohamad & Ghani Rafek, 1993). To date, there has been no publicly available information or data on the REE for the weathered profiles of Taiping pluton. Hence, this paper aims to investigate the geochemical distribution of REE content in the weathered products of Taiping pluton.

Study area

The study area is located at the southern part of Taiping pluton and is divided into three sampling locations (Figure 1). First sampling location, PSS, is located approximately 2.0 kilometres southwest of Kampung Sauk. The second sampling location, PUK, is located approximately 500 metres from Kampung Ulu Kernas. Lastly, the third sampling location, MJ, is located at Madu Jaya Quarry which is located approximately 3.3 kilometres from Kampung Sungai Air Terjun.

MATERIALS AND METHODOLOGY

Soil and rock sampling

A total of 36 representative samples were collected systematically, starting from horizon A (approximately around 0.2m to 0.5m below the surface), and continuing through horizon B, horizon C and the underlying rock (horizon D) (Figure 2). Soil sampling and classification was carried out based on characteristics described by Sanematsu *et al*. (2013). The samples were acquired from three sites, namely PSS, PUK and MJ (Figure 1).

According to Keller (1963), horizon A is composed of dark brown soil. This horizon is rich in organic material, clay minerals and quartz while only containing very small quantities of primary rock – forming minerals. Horizon B is characterised by reduced organic content and displays yellowish to reddish – brown coloration. Granitic textures generally cannot be seen within this horizon. Horizon C is represented by a fragile weathered layer developed on the parent granite, typically displaying yellowish to greyish colour. In this horizon, granitic textures and primary minerals such as feldspars and biotite are still identifiable. The writer also noted that the transition from horizon C to horizon B would occur gradually and without any distinct boundary.

The regolith samples were analysed using X-ray fluorescence (XRF), X-ray diffraction (XRD) and inductively coupled plasma mass spectrometry (ICP-MS). Prior to these geochemical and mineralogical analyses, the samples were air dried, ground using a Fritsch mortar and sieved through 75 micrometre mesh. For the granite samples, in addition to laboratory-based geochemical and mineralogical analyses, thin sections were prepared and examined under a petrological microscope

Laboratory analyses

Geochemical analyses

Geochemical analyses, which include XRF and ICP-MS, was conducted at Bureau Veritas Commodities, Vancouver, Canada. XRF analysis was conducted to obtain the major elemental compositions such as SiO_2, Fe_2O_3, CaO, TiO_2, K_2O, P_2O_5, Na_2O, MnO, and MgO. Loss on ignition (LOI) values were measured in accordance with standard laboratory protocols. The ICP-MS analysis, using a standard analytical procedure, was conducted to obtain the concentration of REEs, U and Th. Total REE (TREE), total light REE (TLREE) and total heavy REE (THREE) were calculated by summing the appropriate values. The minimum, maximum and average values for each element were determined, including TLREE, THREE and TREE, along with the calculation of Ce/Ce*, Eu/Eu* and La/Yb ratio. REE concentrations were normalised to chondritic values using the elemental abundances of (Sun & McDonough, 1989), from which the chondrite-normalised REE plot diagram was constructed.

XRD analysis

XRD analysis was conducted in the Centralised Analytical Laboratory (CAL) at Universiti Teknologi PETRONAS for all samples. The analysis aims to identify the mineral content in the soil and in rock samples. Samples were pulverised to <75µm prior to the analysis. Diffractograms were acquired between 0 and 100 2Θ peaks and the data were then processed using Panalytical's Xpert Highscore Plus™ software.

Petrographic study

All collected rock samples were prepared for petrographic study. The granitic rocks were first cut into rectangular size chips then glued and ground to

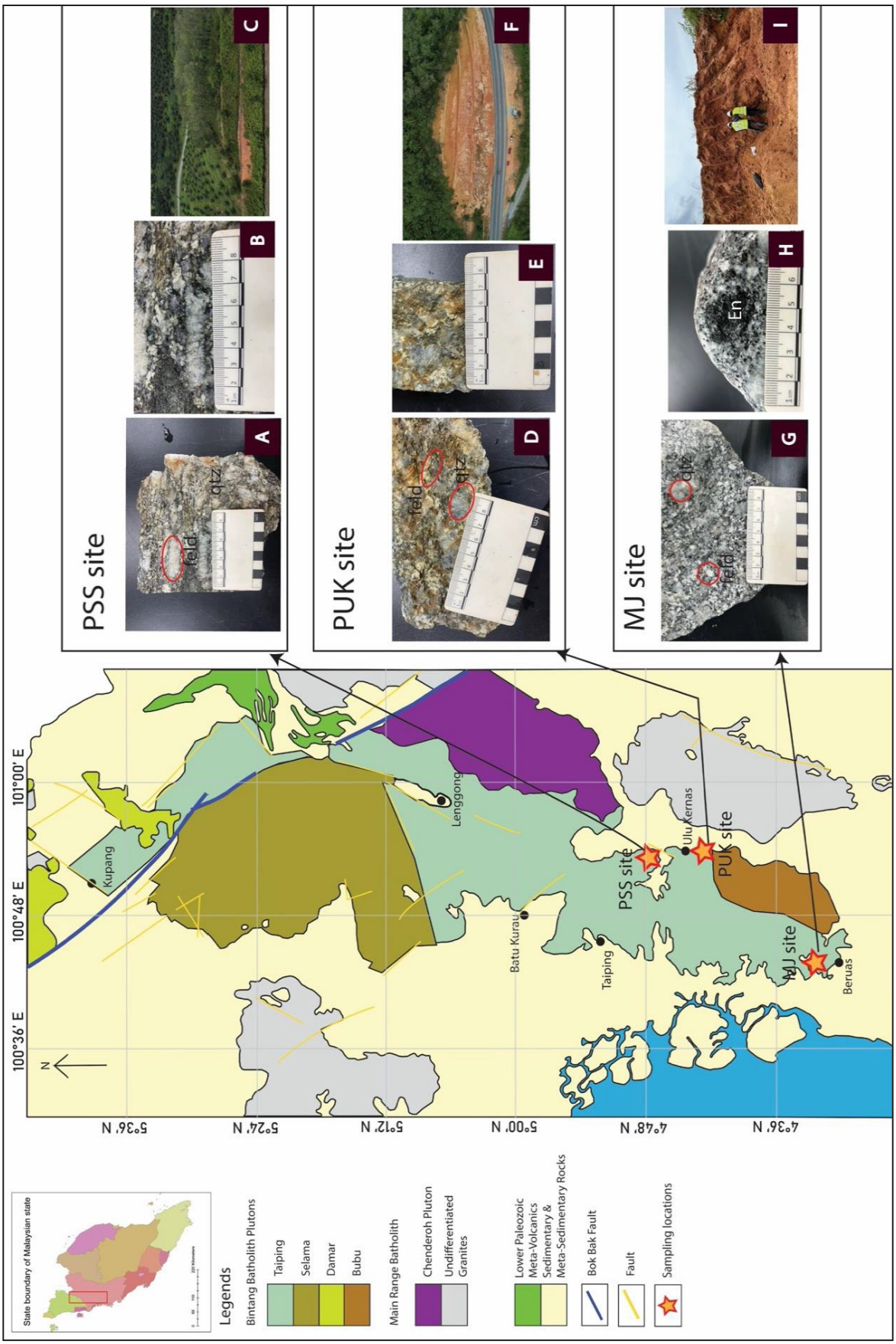

Figure 1: The figure shows the divisions of Taiping pluton, modified from Quek *et al.* (2016). The sampling locations are marked with stars. Feld is feldspar, qtz is quartz, en is enclave.

the thickness of approximately 30 micrometres, or the thickness which is suitable for the microscopic observations.

RESULTS

Field observations

The weathered granite profiles in all 3 sampling sites (PSS, PUK and MJ) range from 7 to 15 metres in thickness. Horizon A (Figure 3) consists of dark brown to reddish brown soil, enriched with plant roots, can be easily crumbled by hand and has thickness ranging from 20 to 50 centimetres.

The B horizon was identified to have yellowish to reddish brown in colour and lacks any visible granitic texture. When moistened, the soil can be rolled between fingers. The presence of feldspar minerals residues is scarce due to its highly weathered nature of horizon B, but they still can be identified with mineral remnants having white colour, contrasting to the colour of matrix. This horizon is highly enriched with clay minerals with little to no organic matter or plant roots.

The C horizon displays a distinctive brown to dark reddish-brown coloration while retaining remnants of its granitic textures. The darker colour likely reflects the melagranitic composition of the Taiping pluton, which is enriched in mafic mineral components. Despite weathering, the primary rock-forming minerals remain identifiable. Compared to the overlying B horizon, the soil material in this layer exhibits reduced plasticity when rolled between the fingers and can be easily disintegrated.

Horizon D, which is the bedrock, can be easily identified from the profile. The bedrock samples are derived from the amphibole-bearing melagranite of Taiping pluton. These samples display quartz and feldspar minerals ranging from 3 cm to 70 cm in length. The mafic microgranular enclaves (MME) observed within the granite are generally only a few centimetres in size and exhibit sharp contacts with the surrounding granitic host rock. At the MJ site, located in the southernmost part of the Taiping pluton, the granite appears noticeably lighter in colour compared to samples collected from more northern areas as noted by Quek *et al*. (2015). Variations in the thickness of the weathered profiles from each site are likely due to erosional processes that thinned out the weathered crusts. On average, the weathered crusts are mostly developed with the thickness of 7 metres.

XRF and Loss on Ignition (LOI) results

The XRF analysis for soil the samples (Table 1) shows that Al_2O_3 content is highest in horizon B for

Figure 2: Exposed weathered granite profiles together with the bedrock at PUK site showing all the horizons.

Figure 3: One of exposed horizon A (left), horizon B (middle) and horizon C (right) profiles.

Table 1: Results of XRF, LOI and ICP - MS analyses for all samples. XRF and LOI results are shown in percentages (%), while ICP – MS results are expressed in parts per million (ppm).

Sample	MJ A	MJ B	MJ C	MJ D	PUK A	PUK B	PUK C	PUK D	PSS A	PSS B	PSS C	PSS D
Horizon	**A**	**B**	**C**	**D**	**A**	**B**	**C**	**D**	**A**	**B**	**C**	**D**
SiO_2	58.06	44.43	58.63	70.30	65.51	59.86	61.17	74.09	62.08	59.64	59.47	66.42
Al_2O_3	22.84	32.14	24.09	14.20	20.33	24.44	23.32	13.99	20.94	23.58	22.50	13.64
Fe_2O_3	3.91	6.96	3.99	2.90	4.49	5.35	5.05	1.59	4.57	5.31	4.56	4.76
K_2O	0.73	0.64	4.08	5.25	0.19	0.20	0.38	5.22	0.11	0.11	5.92	3.60
TiO_2	0.65	1.03	0.64	0.50	0.75	0.73	0.71	0.34	0.76	0.84	0.73	0.84
Na_2O	0.03	<0.01	0.10	2.69	<0.01	<0.01	<0.01	2.87	<0.01	<0.01	0.18	2.03
CaO	0.04	0.03	0.05	2.22	<0.01	<0.01	0.02	1.20	4.57	5.31	4.56	4.76
MgO	0.08	0.13	0.37	1.36	0.02	0.02	0.03	028	0.06	0.06	0.48	3.11
MnO	0.01	0.01	0.02	0.05	0.02	0.02	0.02	0.02	<0.01	<0.01	0.03	0.06
P_2O_5	0.05	0.07	0.11	0.16	0.04	0.02	0.04	0.09	0.05	0.04	0.05	0.33
LOI	13.00	14.80	7.90	0.90	9.10	9.80	9.70	0.90	11.10	9.40	6.10	1.70
Total	99.40	99.60	99.98	99.87	100	100	99.65	99.80	93.14	94.89	98.48	99.55
Sc	5.40	12.80	9.50	6.60	4.10	5.80	7.10	2.60	9.10	10.00	9.90	4.10
Y	3.73	6.16	42.64	22.17	1.91	2.82	4.35	108.05	1.45	1.53	37.05	12.34
La	18.00	34.90	310.60	58.00	12.10	12.50	25.80	80.20	5.20	5.50	136.50	91.20
Ce	138.10	342.60	338.60	122.20	50.90	107.50	297.80	120.60	74.50	177.00	193.10	176.60
Pr	4.27	8.51	71.40	13.98	2.89	2.92	6.21	19.69	1.29	1.34	37.46	19.43
Nd	14.80	27.85	236.13	49.22	10.36	10.58	21.84	76.13	4.91	5.01	140.92	65.72
Sm	2.86	5.50	35.29	8.53	1.87	1.94	3.87	18.09	1.00	0.96	21.64	8.67
Eu	0.18	0.50	3.45	0.29	0.03	0.08	0.11	1.60	0.13	0.13	2.66	0.65
Gd	2.00	3.81	17.58	6.08	1.30	1.49	3.01	19.47	0.74	0.94	12.17	5.20
Tb	0.23	0.45	2.04	0.78	0.14	0.16	0.30	3.19	0.08	0.09	1.44	0.56
Dy	1.16	2.30	10.66	4.23	0.63	0.78	1.39	19.64	0.44	0.44	7.85	2.71
Ho	0.17	0.33	1.74	0.74	0.08	0.12	0.20	3.65	0.07	0.07	1.38	0.44
Er	0.45	0.85	5.04	2.17	0.18	0.30	0.49	10.22	0.20	0.20	4.15	1.21
Tm	0.06	0.11	0.72	0.30	0.02	0.04	0.06	1.29	0.03	0.03	0.58	0.15
Yb	0.38	0.69	5.02	1.99	0.10	0.23	0.36	8.09	0.21	0.21	4.02	0.92
Lu	0.05	0.08	0.66	0.28	0.02	0.03	0.05	1.05	0.03	0.03	0.53	0.13
Th	70.50	115.60	66.60	42.40	62.60	77.50	89.10	25.70	74.80	87.50	69.50	63.80
U	9.50	19.00	19.60	13.50	2.60	3.00	11.80	8.80	5.30	6.00	16.90	10.50
`TLREE	180.21	423.67	1013.05	258.30	79.45	137.01	358.64	335.78	87.77	190.88	544.45	367.47
THREE	6.23	10.97	68.52	32.66	3.08	4.48	7.20	155.18	2.51	5.60	57.00	18.46
TREE	186.44	434.64	1081.57	290.96	82.53	141.49	365.84	490.96	90.28	196.48	601.45	385.93
Ce/Ce*	3.79	4.78	0.55	1.03	2.07	4.27	5.66	0.73	6.92	15.67	0.65	1.01
Eu/Eu*	0.06	0.07	0.01	0.02	0.03	0.06	0.02	0.01	0.36	0.30	0.02	0.03
La/Yb	47.63	50.83	61.98	29.21	121.18	54.52	71.77	9.92	24.80	26.23	34.05	9.24

all sites, with values of 32.14% (MJ B), 24.44% (PUK B) and 23.58% (PSS B). High Al_2O_3 content generally reflects higher concentrations of clay minerals, particularly kaolinite and gibbsite (Keller, 1963). Despite this, high TREE concentrations are found in the C horizon. SiO_2 is generally found in high concentrations in horizon A, ranging from 58.06% to 65.51%. Fe_2O_3 is highest within the B horizon with values ranging from 5.31% to 6.96%. LOI values generally show an increasing trend towards a higher weathering grade soils and are directly proportional to the increasing contents of Al_2O_3.

XRF analysis of the rock samples indicates higher concentrations of SiO_2 (66.42% to 70.30%), CaO (1.20% to 3.59%) and P_2O_5 (0.09% to 0.33%) compared to the soil samples. In contrast, Al_2O_3 (13.64% to 14.20%) and Fe_2O_3 (1.59% to 4.76%) contents are lower in the rock samples.

XRD results

According to XRD analysis results of soil samples (Figure 4), horizon A is dominated by quartz (75% to 78%) with the remainder consisting of clay (22% to 25%). This mineralogical composition is similar in all horizon A from each site, with no other significant minerals present.

In horizon B, quartz content drops to 43% to 54% while the clay content increases to 30% to 46%. At MJ site, gibbsite (27%) is also present. This horizon generally shows a reduction in quartz compared to horizon A, with more secondary minerals appearing.

The MJ C sample shows a balanced mix of minerals with quartz at 31%, clay at 15%, K – feldspar at 30% and vermiculite at 24%. PSS C sample is dominated by K – feldspar (52%) with smaller amount of quartz (22%), followed by clay (16%) and gibbsite (10%). The PUK C sample remains quartz – rich (67%) but also contains clay (23%) and gibbsite (10%). This layer marks the introduction of feldspars and vermiculite, especially prominent at the MJ and PSS sites, within the weathered profiles of Taiping pluton.

The MJ D sample contains quartz (29%), a high proportion of K – feldspar (41%) and biotite (30%). The PSS D sample includes quartz (29%), albite (22%), biotite (17%) and K – feldspar (32%). The PUK D sample is dominated by albite (40%), with quartz (22%), K feldspar (33%) and minor amount of biotite (5%). This horizon is clearly more enriched with feldspars and marks the transition into the parent rock's mineralogy in the study area.

Although hornblende was previously reported in Taiping pluton by Ghani *et al*. (2013), it was not detected in the present XRD analysis. This absence may be due to the low abundance of the mineral in the samples, which may fall below the detection limit of the laboratory's XRD instrument. The same reason explains why the REMs were not detected in the bulk powder analysis of the Taiping pluton samples. REMs present at low concentrations (typically below 1-2 %) might fall below the XRD detection limit and thus remain undetected (Keller, 1963).

ICP-MS results

Results of ICP-MS analysis are shown in Table 1. Analysis of soil samples shows that TREE concentrations for horizon A range from 70.00 ppm to 771.00 ppm, with an average value of 291.00 ppm. These concentrations are dominated by LREE, which range from 67.00 ppm to 702.00 ppm, while HREE are significantly lower, ranging from 2.51 ppm to 155.00 ppm. Notably, the MJ C soil sample recorded the highest TLREE content, dominated by Ce, Nd, and Pr.

Thorium (Th) concentrations in the soil samples range from 62.60 ppm to 115.60 ppm, while uranium (U) contents vary between 2.60 ppm and 16.90 ppm. Among the samples, MJ B has the highest Th content, whereas MJ C shows the highest U concentration.

ICP-MS analysis of the rock samples reveals TREE values between 233.00 ppm and 411.00 ppm, with an average of 313.00 ppm. Similar to the weathered profiles, the LREE are more abundant than the HREE. TLREE concentration ranges from 200.00 ppm to 276.00 ppm,

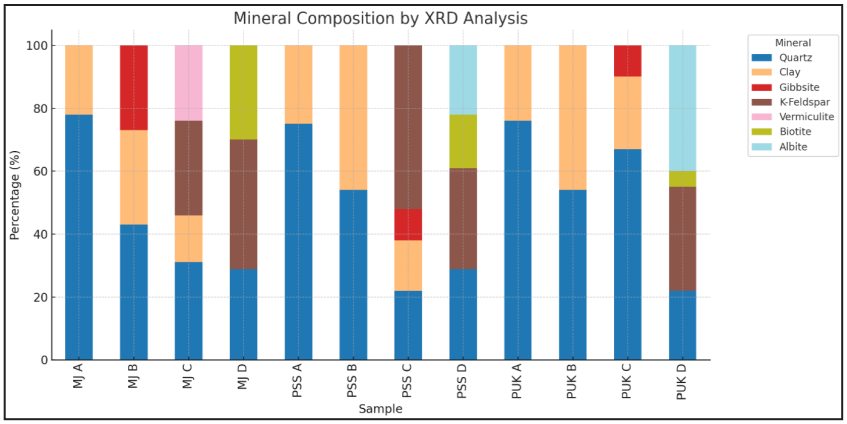

Figure 4: Results of XRD analyses for each sample.

whereas THREE values range between 18.00 ppm and 155.00 ppm. In the rock samples, Th contents range from 25.70 ppm to 63.80 ppm, while U contents range from 8.80 ppm to 13.50 ppm. PSS D and MJ D contain highest Th and U concentrations, respectively.

Chondrite-normalised plot

The chondrite-normalised REE patterns (Figure 5) are derived from the ICP-MS analysis results. The plotted patterns show generally the same variations between the fresh rock and the overlying weathered products of the Taiping pluton. Negative Eu anomalies are observed in both rock and soil samples of the Taiping pluton. The Ce anomalies, in contrast, shows positive anomalies for all samples, except for horizon C samples from MJ and PSS sites.

The positive Ce anomalies are likely attributed to the oxidation of Ce^{3+} to the less soluble Ce^{4+} under near surface oxidative conditions, before being adsorbed onto secondary clay minerals. In this study, Ce enrichment occurs in horizon C and negative Ce anomalies can be observed within C horizons at all localities, except for the PUK site, while other samples are showing positive Ce anomalies.

The La/Yb ratio shows higher values in the soil samples compared to the rock samples.

Petrographic study

The micro-scale images from mineralogical studies of the Buloh Pelang unit, under the petrological microscope, are shown in Figure 6. As the sites are hosted on the same bedrock, the mineral contents are generally consistent, comprising quartz, K-feldspar, plagioclase and biotite as the dominant minerals. Hornblende can be observed in the MJ rock sample as an accessory mineral while REMs like zircon and apatite occur as inclusions within biotite. All the rock samples have the same REMs contain within them, which are apatite and zircon. Textures indicative of radiation damage (or metamictisation) in biotite was observed, such as the presence of a black halo around zircon inclusions. The metamictisation process will cause the mineral textures to be destroyed and creates zoning appearance due to the high abundance of radioactive elements within the zircon (Yaraghi *et al*., 2020).

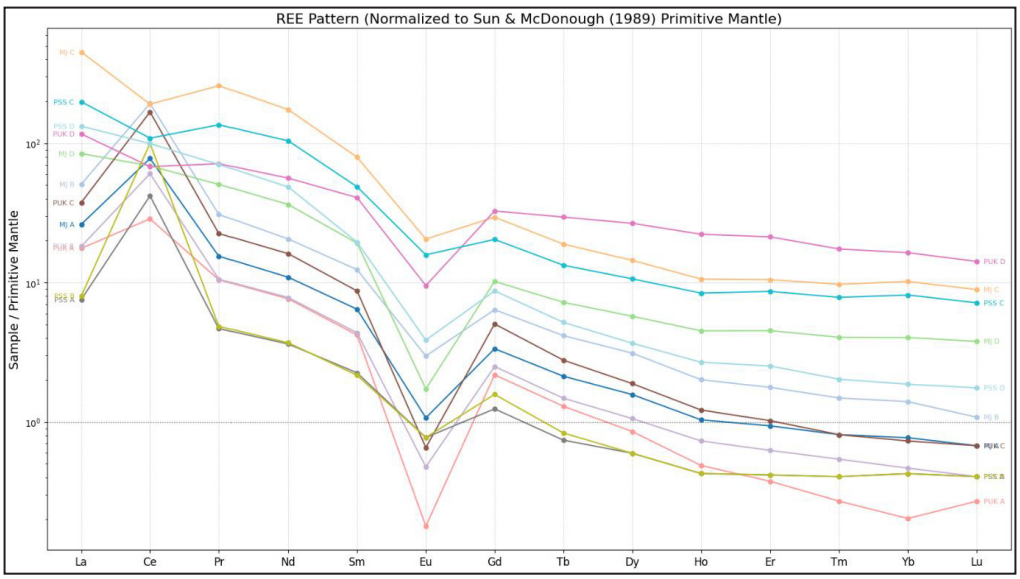

Figure 5: Chondrite - normalised diagram for REE concentrations for each sample. Details of concentration for each sample are given in Table 1.

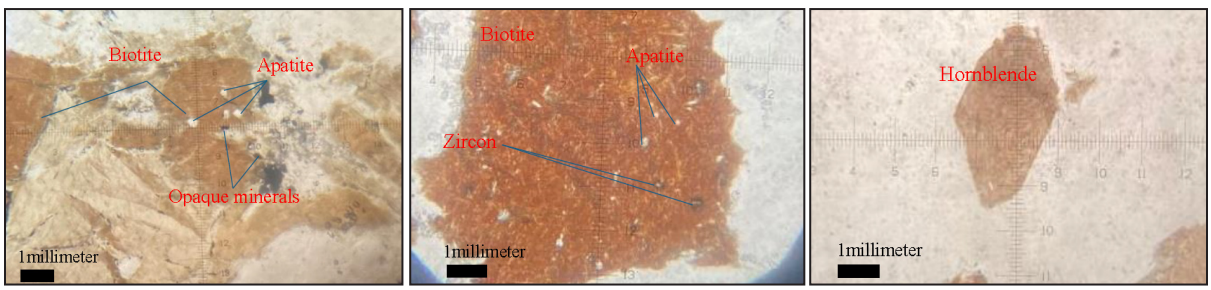

Figure 6: Thin section images from PSS D (left), PUK D (middle) and MJ D (right), as viewed under plan-polarised light.

Among the observed REMs, apatite is the most likely source of REE enrichment within the weathered profiles. Although it occurs as an inclusion within biotite, it has higher solubility, especially in acidic to slightly acidic pH environments, making it prone to breakdown and LREE release during weathering processes. In contrast, zircon with high resistance to chemical weathering, contributes minimally to REE release.

Although zircon can be observed in thin sections of the rock samples, the REE distribution patterns, as shown in Figure 5, are LREE-enriched with no HREE peaks. This indicates that apatite is the primary source for the REE enrichment in the profiles.

DISCUSSION

Weathering profile development

The variation in horizon thickness and mineralogical composition across the three sites reflects the different duration of exposure towards weathering processes within the Taiping pluton. The gradual transition from horizon A that are rich in quartz to clay-rich B horizons and feldspar-bearing C-horizons proves the progressive decomposition of the silicate minerals, consistent with the classical granite weathering sequence described by Keller (1963). Higher Al_2O_3 and LOI contents in the soil horizons also reflect significant chemical weathering, where K-feldspar and plagioclase are weathered into clay minerals under reducing conditions (Yaraghi *et al*., 2020). The darker coloration in horizon B and C corresponds to the melagranitic composition of the parent rock, which contains proportions of mafic minerals hence making the horizon to be enriched with dark minerals.

Enrichment patterns across horizons

Observed chondrite-normalised REE patterns show enrichment of LREE over HREE across all horizons. This fractionation indicates that the LREE are more mobile and released during the weathering of lower resistant REM such as apatite, while HREE remain immobile as the more resistant REM such as zircon are less affected during weathering processes. The highest TREE values can be found in C horizon, moderate in B horizon and lowest in A horizon. This suggests a downward migration and accumulation of REE near the weathering front.

Based on the ICP-MS results, horizons with negative Ce anomalies are showing higher TREE contents compared to soil horizons with positive Ce anomalies, in the Taiping pluton's weathered profile. The overall pattern of Ce anomalies is consistent with the finding of Sanematsu *et al*. (2013), who noted that positive anomalies of Ce are characteristics of shallow leaching zones of REE, while negative Ce anomalies typically develop in deeper in deeper horizons where REE accumulates. The enrichment of REE within the weathered profiles is primarily attributed from the weathering of apatite. This process results in significant enrichment of LREE relative to HREE, as observed in chondrite-normalised pattern, which display absence of distinct HREE peaks.

Eu anomalies are found to be uniformly negative across all samples, indicating a strong depletion in Eu content. Eu^{2+} typically substitutes for Ca^{2+} in plagioclase during crystallisation, resulting in preferential partitioning of Eu into feldspar (Compton *et al*., 2003). Feldspar is then removed via fractional crystallisation processes during magma evolution, leading to the negative anomalies characteristics of granites (Duzgoren-Aydin & Aydin, 2009). Therefore, the negative Eu anomaly in the weathered profiles of the Taiping pluton reflects the original magmatic differentiation history of the parent rock, rather than being produced by later weathering processes.

As for the La/Yb ratio, it is found that the ratio is higher in the weathered materials compared to rock. According to Sanematsu *et al*. (2013), this is indicative of LREE are more enriched compared to HREE.

CONCLUSION

The decisive factor that controls the enrichment of LREE and HREE during rock weathering is primarily governed by the presence of REM and their susceptibility to alteration. This study investigated weathering profiles derived from the amphibole – bearing granite of the Taiping pluton. Sampling was conducted along vertical profiles at three different localities, and the samples were subjected to characterisation using geochemical analyses, XRD and petrographic analyses (rock samples only).

The weathering crust is divided into four main horizons. Horizon A is an organic-rich layer enriched with plant roots. Horizon B is dominated by clay with no obvious relict granite structures while horizon C is differentiated by the presence of identifiable relict or weathered rock – forming minerals from the Taiping pluton. Horizon D represents the unweathered granite bedrock. Petrographic analyses confirmed the presence of apatite and zircon, with apatite being the likely source of REE release during weathering. Metamictisation is observed around zircon inclusions. The radiation effect can be seen on biotite mineral, and it is due to the high content of radioactive elements within the zircon itself.

Based on the XRF results, SiO_2 together with Al_2O_3 are found to be the most abundant oxides in all analysed samples. XRD analyses show that quartz is present in all collected samples. Secondary minerals, such as clay, gibbsite and vermiculite, are present in the weathered profiles of the Taiping pluton.

Based on the ICP-MS analysis results, TREE is the highest at 490.96 ppm in PUK site for the rock sample. The average TREE for the three sampled Taiping pluton rocks is 389.28ppm. For the soil samples, it is observed that REE is concentrated at the lower weathering profile. It is likely due to the continuous REE supply from apatite

weathering near the bedrock zone. Horizon C has an average TREE concentration of 682.95 ppm, while horizon B and horizon A have average TREE concentrations of 257.54 ppm and 119.75 ppm, respectively. The high TREE content in horizon C is most likely due to the horizon being deeper, which makes it closer in proximity to the bedrock and to the REMs. The ICP-MS results show good corresponding to the findings of (Sanematsu *et al*., 2013), who reported REE enrichment is observed to occur within soil horizons characterised with negative Ce anomalies.

Future investigations should incorporate advanced techniques such as LA-ICP-MS for mineral characterisation and leaching experiments to evaluate REE mobility within horizons.

ACKNOWLEDGEMENT

My highest appreciation to Universiti Teknologi PETRONAS (UTP) and Yayasan UTP Universiti Teknologi PETRONAS (YUTP – FRG – 015LC0 – 433, YUTP – FRG – 015LC0 – 081, and YUTP – FRG – 015LC0 – 305) for providing me the instruments and resources required for this research, to all the staff of Geoscience Department of UTP, and the anonymous reviewers for the suggestions and comments which have helped me to improve the quality of my article.

AUTHORS CONTRIBUTION

IDM, NSZA and BCB contributed to the field sampling activities. Sample preparations, data analysis and interpretations were performed by IDM. IDM wrote the whole manuscript, NSZA and BCB contributed ideas to improve the paper.

CONFLICT OF INTEREST

The authors declare there is no conflict of interest.

REFERENCES

Akademi Sains Malaysia, 2014. Blueprint for the establishment of rare earth-based industries in Malaysia: a strategic new source for economic growth. Akademi Sains Malaysia: Ministry of Science, Technology and Innovation, Kuala Lumpur. 218 p. ISBN 978-983-9445-947.

Compton, J.S., White, R.A., & Smith, M., 2003. Rare earth element behavior in soils and salt pan sediments of a semi-arid granitic terrain in the Western Cape, South Africa. Chemical Geology, 201, 239–255.

Duzgoren-Aydin, N.S., & Aydin, A., 2009. Distribution of rare earth elements and oxyhydroxide phases within a weathered felsic igneous profile in Hong Kong. Journal of Asian Earth Sciences, 34, 1–9.

Ghani, A.A., 2005. Geochemical characteristics of S- and I-Type Granites : Example From Peninsular Malaysia Granites. Bulletin of the Geological Society of Malaysia, 51, 123-134.

Ghani, A.A., Searle, M., Robb, L., & Chung, S. L., 2013. Transitional I S type characteristic in the Main Range Granite, Peninsular Malaysia. Journal of Asian Earth Sciences, 76, 225–240.

Haxel, G.B., Hedrick, J.B., & Orris, G.J., 2002. Rare Earth Elements—Critical Resources for High Technology. U.S Geological Survey Fact Sheet, 087-02.

Husin, Z., Ab. Ghani, M.Z., Abdul Rahman, A.H., Eki, A., Ariffin, H. K.M., Ibrahim, I., & Ibrahim, K. & J. J. J., 2015. Guidelines rare earth element explorations. Department of Mineral and Geosciences Malaysia, Kuala Lumpur. 80 p. (in Malay).

Ibad, S.M., Tsegab, H., Siddiqui, N.A., Adam, M., Mishra, S., Ridha, S., Ahmed, N., & Azmi, A., 2024. The upstream rare earth resources of Malaysia: Insight into geology, geochemistry, and hydrometallurgical approaches. Geoscience Frontiers, 15(6), 101899. https://doi.org/10.1016/j.gsf.2024.101899.

Keller, D., 1963. The Origin Of High-Alumina Clay Minerals-A Review. Clays Clay Mineral, 12, 129-151.

Malaysian Meteorological Department, 2025. Malaysia's Climate. Ministry of Natural Resources and Environmental Sustainability.

Mohamad, H., & Ghani Rafek, A., 1993. The distribution of rare earth elements in tropical granitic soil: a case study from Malaysia. Journal of Southeast Asian Earth Sciences, 8, 617 – 625.

Mouchos, E., Wall, F., Williamson, B.J., & Palumbo-Roe, B., 2017. Easily Leachable Rare Earth Element Phases In The Parnassus-Giona Bauxite Deposits, Greece. Bulletin Of The Geological Society Of Greece, 50, 1952-1958.

Quek, L.X., Ghani, A.A., Chung, S.L., Li, S., Lai, Y.M., Saidin, M., Amir Hassan, M.H., Muhammad Ali, M.A., Badruldin, M.H., & Abu Bakar, A.F., 2017. Mafic microgranular enclaves (MMEs) in amphibole-bearing granites of the Bintang batholith, Main Range granite province: Evidence for a meta-igneous basement in Western Peninsular Malaysia. Journal of Asian Earth Sciences, 143, 11–29.

Quek, L.X., Ghani, A.A., Saidin, M., & Harith, Z.Z.T., 2016. Durbachite-like melagranite in Taiping pluton of Bintang Batholith, Peninsular Malaysia. Bulletin of the Geological Society of Malaysia, 62, 1–6.

Quek, L.X., Jamil, A., Ghani, A.A., & Saidin, M., 2015. Highly potassic melagranite of Bintang Batholith, Main Range Granite, Peninsular Malaysia. Current Science, 108, 2159–2163.

Sanematsu, K., Kon, Y., Imai, A., Watanabe, K., & Watanabe, Y., 2013. Geochemical and mineralogical characteristics of ion-adsorption type REE mineralization in Phuket, Thailand. Mineralium Deposita, 48, 437–451.

Sun, S.S., & McDonough, W.F., 1989. Chemical and isotopic systematics of Oceanic Basalts: Implications for mantle composition and processes. In: Saunders, A.D. & Norry, M.J. (Eds.), Magmatism in the Ocean Basins. Geological Society London Special Publications, 42(1), 313–345. https://doi.org/10.1144/GSL.SP.1989.042.01.19.

Yaraghi, A., Ariffin, K.S., & Baharun, N., 2020. Comparison of characteristics and geochemical behaviors of REEs in two weathered granitic profiles generated from metamictized bedrocks in Western Peninsular Malaysia. Journal of Asian Earth Sciences, 199, 104385. https://doi.org/10.1016/j.jseaes.2020.104385.

Manuscript received 2 June 2025;
Received in revised form 23 August 2025;
Accepted 23 December 2025
Available online 30 April 2026